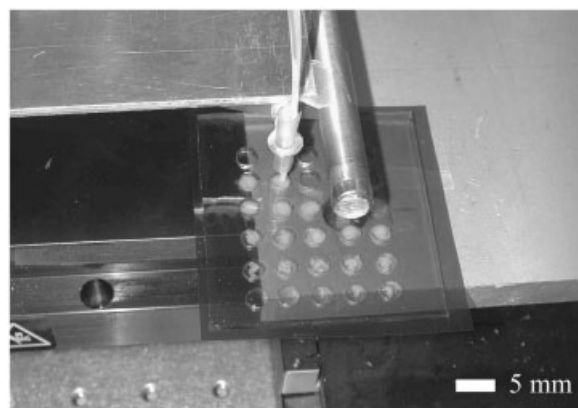


**Summary:** We present a high throughput X-ray scattering study (SAXS/WAXS) of the formation and stability of the vesicle phase of a water soluble diblock copolymer. The vesicle shape and shell thickness were investigated as a function of block copolymer concentration and temperature. We were able to establish a growth in the SAXS peak as concentration increased, indicating a greater polymer concentration of vesicles. The effect of temperature was also investigated.

Library sample of a discrete concentration gradient of EO(6)BO(11) in water.



## Scattering Measurements for High Throughput Materials Science Research<sup>a</sup>

Alexander I. Norman,\* João T. Cabral, Alamgir Karim, Eric J. Amis

Polymers Division, National Institute of Standards and Technology, 100 Bureau Drive, Gaithersburg, Maryland, 20899-8542, USA  
Fax: +1 301 9754924; E-mail: alexander.norman@nist.gov

Received: October 27, 2003; Revised: November 5, 2003; Accepted: November 6, 2003; DOI: 10.1002/marc.200300239

**Keywords:** combinatorial; diblock copolymers; phase behavior; SAXS; WAXS

### Introduction

High throughput scattering methods were employed to study phase behavior over a concentration gradient to probe the vesicle structure of a diblock copolymer in water. Combinatorial approaches use composition libraries, either continuous gradients or discrete multiple samples removing the need for preparing each individual sample and reducing experimental acquisition time, since the samples do not need to be loaded individually, and no re-alignment procedures are required. In this work, scattering methods were chosen to study such systems, since they cover length scales ranging from a few angstroms (WAXS – Wide angle X-ray scattering) to approximately 200 nm (SAXS – Small angle X-ray scattering). Moreover, since the structure is probed in reciprocal space and the inspection volumes are large compared to the scattering units, representative statistical properties are obtained without local artifacts. In addition,

this technique is nondestructive and data acquisition is rapid, typically 10 to 150 s, dependent on flux, the count rate of the detectors, and the degree of contrast. To carry out such experiments as quickly as possible, all SAXS/WAXS studies are carried out at a synchrotron source, where the flux is significantly higher than conventional laboratory sources, typically  $10^{11}$  to  $10^{13}$  photons/s, and the wavelength is monochromatic, typically 0.8 to 1.5 Å.

Liquid composition libraries can be prepared by three different methods. (1) A time variant device consisting of inlet and outlet channels, which different components are pumped through, to give a variation in concentration with time.<sup>[1]</sup> (2) A continuous concentration gradient, which is prepared by means of a flow coater.<sup>[2]</sup> However, this technique is only suitable for thin films, where confinement and surface attraction may modify phase behavior, and requires negligible diffusion during sampling times. It has therefore limited applicability when designing libraries for scattering experiments in the bulk. We have therefore used a (3) discrete composition gradient, consisting of a multiwell library, each well containing varying amounts of each component. By incorporating such a library into scattering

<sup>a</sup> Official contribution of the National Institute of Standards and Technology; not subject to copyright in the United States.

experiments, we can rapidly probe the structure over a large number of concentrations by scanning a collimated X-ray beam through the multiple sample array. In this work, we used a 25-well array (with sample volume  $\approx 150 \mu\text{L}$ ), spanning concentrations from 0 to 20% by mass fraction in increments of 0.8% for demonstration purposes.

## Experimental Part

### Sample Preparation

A sample of poly(ethylene oxide-*block*-butylene oxide), EO(6)BO(11) (where EO denotes an ethylene oxide unit and BO denotes a butylene oxide unit), was obtained from the Dow Chemical Company and used as received.<sup>[4]</sup> Details of the synthesis and characterization techniques can be found in the literature.<sup>[3]</sup> A 20% solution of the block copolymer in de-ionized water was prepared, mechanically agitated for 30 s, and allowed to stand for a minimum of 24 h before examination. On inspection, the sample appeared opaque at room temperature.

Harris et al.<sup>[3]</sup> established that the vesicle phase of this copolymer is stable at room temperature up to concentrations of 20%; hence, we study this system by SAXS/WAXS over the whole concentration window from 0 to 20%, incorporating 25 samples within this range.

The discrete composition gradient was fabricated using an in-house built liquid dispenser and deposited on a multiwell substrate. The liquid dispenser consists of a series of syringe pumps (New Era, NY), an XY stage (composed of two orthogonal stacked linear stages, ILS150CC Newport, CA), and a motorized actuator along the Z-axis (850G, Newport, CA).<sup>[4]</sup> The syringes are connected with flexible tubing (Tygon 1.5875 mm ID)<sup>[4]</sup> to stainless steel needles (gauge 22), which are attached and mounted onto the Z-actuator, which is normal to the substrate aligned on the XY stage. The syringe pumps and the motion stages are connected to a desktop computer and controlled through a LabVIEW (National Instruments, TX) interface.<sup>[4]</sup> Multicomponent mixtures can be readily prepared within minutes using this technique.

Sample substrates can be designed and fabricated using a recently developed rapid prototyping technique based on the contact lithography of photo-polymerizable resins.<sup>[5,6]</sup> The method requires a 365 nm (UVA) ultraviolet source, a mask printed onto a transparency, and a commercially available optical adhesive. It can produce tall (up to several mm) structures within minutes, which are impervious to a broad range of solvents. Substrates are typically fabricated on glass (for optical transmission) or silicon (for reflection). For this study, a pattern with 25 posts (5 mm diameter) in a squared array was fabricated on glass and its negative was obtained by poly(dimethylsiloxane) PDMS replication (10:1 mass ratio, Sylgard 184, Dow Corning<sup>[4]</sup>).<sup>[5,7]</sup> The result is a perforated PDMS sheet (2 mm thick), which is reversibly sealed within (125  $\mu\text{m}$  thick) polyimide sheets (Kapton, Dupont, OH<sup>[4]</sup>) after being filled with the binary composition library. An earlier version of the PDMS membrane was fabricated by manually punching holes through the elastomer. Kapton provides an effective X-ray scattering window due to its rigidity, high transmission, and low background scattering. PDMS emerges

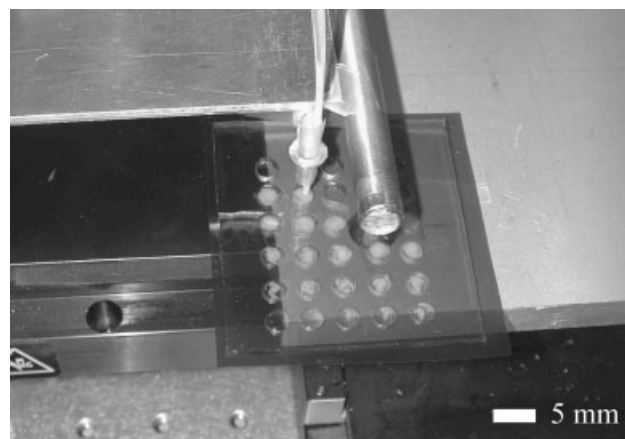


Figure 1. Library sample of a discrete concentration gradient of EO(6)BO(11) in water.

as a suitable gasket material because of its impermeability to water, adhesion to a variety of surfaces (including Kapton) and high molding fidelity.<sup>[8]</sup>

Figure 1 shows the discrete composition library being prepared using the home-built liquid dispenser as described above.

### Simultaneous SAXS/WAXS

SAXS/WAXS measurements were performed on beamline X27C of the National Synchrotron Light Source at the Brookhaven National Laboratory. The beamline was configured for simultaneous SAXS/WAXS experiments using monochromatic radiation of wavelength,  $\lambda = 1.366 \text{ \AA}$ , corresponding to an energy of 10 keV. The evacuated beampipe was equipped with a 1D gas-filled wire small angle detector located 1.944 m from the sample position. A 1D detector is sufficient for such systems as there are no orientation effects, i.e., the scattering is isotropic. In addition, a 1D detector allows more frames to be collected in one single experiment than a 2D area detector. The wide angle detector was placed approximately 10 cm away from the sample at an angle of  $60^\circ$ . Further details of beamline instrumentation, concerning the details on optics, data acquisition, collimation and camera geometry can be found elsewhere.<sup>[9]</sup>

The  $5 \times 5$  sample array was held vertically in front of the beam and clamped in position. A motorized translation stage allowed the movement of the cell to be controlled externally. An exposure time of 120 s for each sample was performed, resulting in 25 SAXS/WAXS data sets over the whole vesicle concentration range to be probed in less than 1 h.

The scattering pattern from silver behenate is used as the small angle diffraction standard. The long spacing of silver behenate,  $d_{001} = 58.380(3) \text{ \AA}$ .<sup>[10]</sup> Higher orders of reflection are seen in the SAXS from this standard and show regular spacing, hence allowing the conversion from pixel number to scattering vector,  $q$ , from Equation (1).

$$q = 2n\pi/d \quad (1)$$

where  $n$  is the order of reflection, and  $d$  is the long spacing and:

$$q = [(4n\pi/\lambda) \sin(\theta/2)] \quad (2)$$

$\lambda$  being the wavelength of the incident beam, and  $\theta$  being the scattering angle. For the WAXS calibration,  $\text{Al}_2\text{O}_3$  was used to convert pixel number into either  $q$  or  $2\theta$ . An exposure time of 60 s was employed for both cases. Two ionization chambers were placed either side of the sample cell to record the incident and transmitted intensity of the X-ray beam. This is used to correct for the transmission of the beam. A detector response measurement was also performed using a  $^{55}\text{Fe}$  radioactive source for approximately 1.5 h. This corrects for any non-linearity of the detectors used. Finally, a background subtraction was recorded; this being the solvent alone held in one of the wells of the library prepared.

In addition to the investigation of the library prepared, temperature ramp experiments using a brass liquid cell (containing polyimide windows) with a water bath temperature control were performed. The sample was heated from room temperature to  $80^\circ\text{C}$  at  $1^\circ\text{C} \cdot \text{min}^{-1}$ . Thirty frames of data were collected, each frame being 120 s, separated by a dead time of  $5 \mu\text{s}$  per frame.

## Results and Discussion

Figure 2 shows the SAXS profiles as a function of concentration of EO(6)BO(11) in water. The units of the scattered intensity are on an arbitrary scale. The absolute calibration of intensity is not required since this is nonessential for the measurement of peak position only. The figure shows how the SAXS profile changes across the concentration gradient library. A broad SAXS peak develops as the concentration is increased indicating that

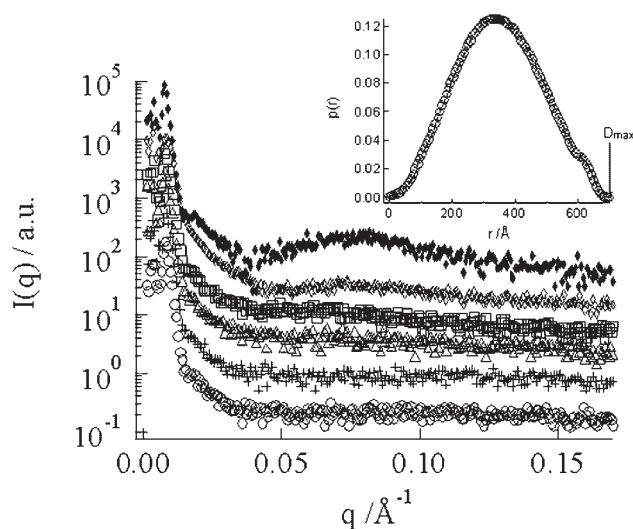


Figure 2. SAXS profiles of EO(6)BO(11) at various concentrations. ( $\circ$  –1.6% (mass fraction),  $+$  –2.4%,  $\triangle$  –3.2%,  $\square$  –4.0%,  $\diamond$  –7.2%,  $\blacklozenge$  –13.6%) at  $22^\circ\text{C}$ . Inset displays the  $p(r)$  function for 13.6% mass fraction of polymer. Uncertainty in  $q$  is  $\pm 0.0005 \text{ \AA}^{-1}$ . Uncertainty in  $p(r)$  is  $\pm 5\%$ .

larger vesicles are present in the system as the concentration increases. The broadness of the SAXS peak is due to the curvature of the lamellar structure, since the bilayers are not as well-correlated as that for a planar lamellar system. A planar lamellar structure results in a more resolved SAXS peak.<sup>[11]</sup> The high intensity at low  $q$  values is due to the scattering around the beamstop and is not a correlation peak. It can be seen that the principle peak position moves to larger  $q$  values as the concentration increases; hence, the domain spacing between lamellae *within* the multilamellar vesicle decreases (e.g.,  $102 \text{ \AA}$  at 4.0% compared to  $77 \text{ \AA}$  at 13.6%). The SAXS spectra were evaluated using an indirect Fourier transformation, which has been described elsewhere.<sup>[12]</sup> Using this technique, particle shape and dimension is obtained from the pair-distance distribution function,  $p(r)$ , which is a function in real space. The inset of Figure 2 reveals the  $p(r)$  function for 13.6% polymer solutions, which is characteristic of a spherical structure.<sup>[13]</sup> One may expect that this function indicates the presence of spherical micelles, however, due to the maximum particle dimension obtained ( $D_{\text{max}}$ ) of  $700 \text{ \AA}$ , we can conclude that this is too large for any micelles formed from such a block copolymer, which are typically in the range of 100 to  $200 \text{ \AA}$  in diameter.<sup>[14]</sup> We therefore conclude that the structures formed are large spherical lamellae, i.e., vesicles. It is noted that the most probable radius of the vesicle is  $320 \text{ \AA}$  from the  $p(r)$  function.

Figure 3 displays the WAXS profile over the concentration range investigated. The data has been shifted along the y axis for clarity. No sharp Bragg peaks are evident, indicating that the system has very little or no crystallinity present. The broad peak over this range is due to the amorphous

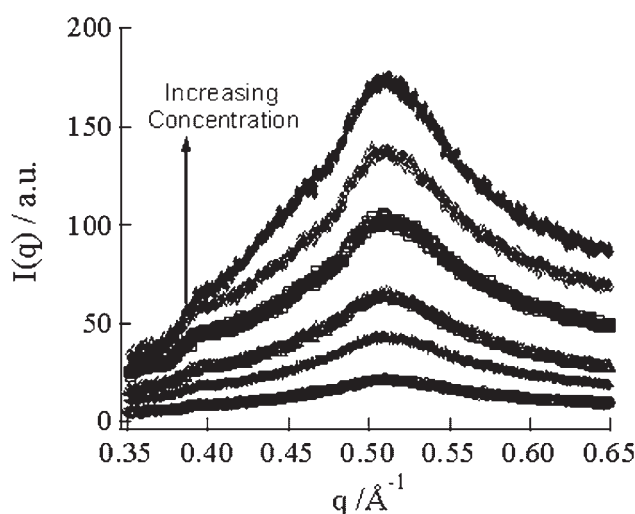


Figure 3. WAXS profile for a range of concentration of EO(6)BO(11) at  $22^\circ\text{C}$  ( $\circ$  –1.6% (mass fraction),  $+$  –2.4%,  $\triangle$  –3.2%,  $\square$  –4.0%,  $\diamond$  –7.2%,  $\blacklozenge$  –13.6%) Uncertainty in  $q$  is  $\pm 0.0005 \text{ \AA}^{-1}$ .



scattering from the local structure and remains the same for each concentration. This implies that the opaque appearance of the samples is due to very large vesicular structures rather than phase separation of polymer from aqueous solvent. Phase separation would also display a distinct high intensity peak in the SAXS profile.

In addition to the concentration gradient library prepared, the temperature dependence of these systems was also carried out using standard SAXS/WAXS techniques.

The most obvious changes are illustrated when a 20% mass fraction sample of polymer is heated from 25 to 80 °C, shown in Figure 4. The inset shows the integrated SAXS intensity (over the  $q$ -range 0.025 to 0.125 Å<sup>-1</sup>) as a function of temperature. The integrated SAXS intensity,  $Q$ , is given as  $Q = \int_{q_1}^{q_2} I(q) dq$ . At 30 °C, the vesicle structure is shown to persist, given by the broad SAXS peak and the spherical  $p(r)$  function. At 40 °C, there is a slight increase in scattered intensity in the region of interest. This indicates that the vesicles have become packed closer together, which is due to the increase in volume of the vesicle and hence, an increase in contrast. The vesicle increases in volume, because as the temperature is increased, water becomes a poorer solvent for the PEO head groups, and to compensate for this, the volume increases. This behavior continues up to 60 °C, at which there is a substantial decrease in scattered intensity; we attribute this to the destruction of the vesicle structure, thus a decrease in contrast. At 70 °C, there is a sudden increase in SAXS intensity, combined with the appearance of three peaks in the ratio 1:√3:√4 with respect to the first order of reflection ( $d = 136$  Å). This relates to an increase in volume fraction of polymer, since the structure

formed is more closely packed than the vesicular structure. The appearance of such peaks in this ratio implies that the structure formed is a hexagonal, lyotropic liquid crystalline array of rod-like micelles.<sup>[11]</sup>

## Conclusion

We have successfully identified the vesicle phase and how it changes as a function of composition and temperature over the concentration region of 0 to 20% mass fraction. With compositions greater than 20%, lyotropic liquid crystal phases form,<sup>[3]</sup> which have not been investigated here, since the formation of such morphologies is well understood.<sup>[15]</sup> The multiwell sample library and automated acquisition used provide invaluable acceleration of the sample inspection.

The development of a novel multiwell heating stage now allows these systems to be studied in a high throughput way as a function of temperature using both in-house small angle light scattering (SALS)<sup>[16]</sup> and SAXS/WAXS, covering an even broader length scale window (≈300 nm to 2 μm).

**Acknowledgements:** We would like to thank *Igors Sics* at the *National Synchrotron Light Source* at *Brookhaven National Laboratory* and *Sheng Lin Gibson* at the *National Institute of Standards and Technology* for their kind assistance during the SAXS/WAXS experiments. We are grateful to *Kapeeshwar Krishana* (at *Rhodia*) for his assistance in setting up the liquid dispenser.

Research carried out (in whole or in part) at the *National Synchrotron Light Source*, *Brookhaven National Laboratory*, which is supported by the *U.S. Department of Energy*, *Division of Materials Sciences and Division of Chemical Sciences*, under Contract No. DE-AC02-98CH10886.

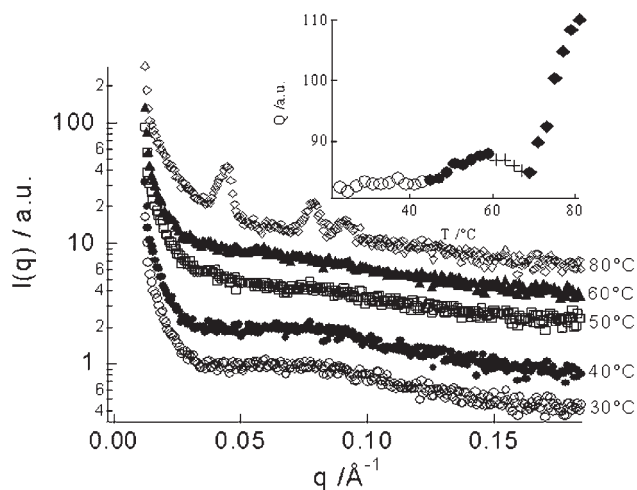


Figure 4. SAXS profiles over a range of temperatures for 20% mass fraction EO(6)BO(11) in water. Inset displays the integrated SAXS intensity over each temperature. Markers indicate the four regimes at which a change in structure appears (see text). (The uncertainty in  $I(q)$  is a result of the uncertainty in wavelength, detector count rate, and back ionization chamber count. These errors are extremely small and have not been quoted).

- [1] H. Song, J. D. Tice, R. F. Ismagilov, *Angew. Chem. Int. Ed.* **2003**, 42, 768.
- [2] J. C. Meredith, A. Karim, E. J. Amis, *Macromolecules* **2000**, 33, 5760.
- [3] J. K. Harris, G. D. Rose, M. L. Bruening, *Langmuir* **2002**, 18, 5337.
- [4] Certain commercial equipment, instruments, or materials are identified in this paper in order to specify the experimental procedure adequately. Such identification is not intended to imply recommendation or endorsement by the National Institute of Standards and Technology, nor is it intended to imply that the materials or equipment identified are necessarily the best available for the purpose.
- [5] C. Harrison, J. T. Cabral, C. M. Stafford, A. Karim, E. J. Amis, *J. Micromech. Microeng.* **2004**, 14, 153.
- [6] J. T. Cabral, unpublished results.
- [7] D. C. Duffy, J. C. McDonald, O. J. A. Schueller, G. M. Whitesides, *Anal. Chem.* **1998**, 70, 4974.
- [8] J. C. McDonald, G. M. Whitesides, *Acc. Chem. Res.* **2002**, 35, 491.
- [9] <http://www.bnl.gov/nsls/x27c/apprt.htm>

- [10] T. C. Huang, H. Toraya, T. N. Blanton, Y. Wu, *J. Appl. Cryst.* **1993**, 26, 180.
- [11] A. I. Norman, J. P. A. Fairclough, S. Mai, A. J. Ryan, *J. Macromol. Sci., Phys.* **2004**, 43, 71.
- [12] B. Weyerich, J. Brunner-Popela, O. Glatter, *J. Appl. Cryst.* **1999**, 32, 197.
- [13] O. Glatter, "The Inverse Scattering Problem in Small-Angle Scattering", in *Neutrons, X-rays, and Light: Scattering methods applied to soft condensed matter*, P. Lindner, T. Zemb, Eds., Elsevier, Amsterdam 2000, p. 82.
- [14] A. I. Norman, D. L. Ho, J. K. Harris, A. Karim, E. J. Amis, *Langmuir*, submitted.
- [15] I. W. Hamley, S. Mai, A. J. Ryan, J. P. A. Fairclough, C. Booth, *Phys. Chem. Chem. Phys.* **2001**, 3, 2972.
- [16] A. I. Norman, unpublished results.